## DISCUSSION

**Y. N. Chen,[1] U. Haupt,[2] U. Seidel,[2] and M. Rautenberg[2]**

The experimental results of this valuable paper reveal a series of very important features of the inception mechanism of rotating stall. They are as follows:

1 The leakage jet, which can be clearly seen from the flow patterns at the normal operating point of $\phi = 0.5$ in Figs. 3(*a*) and 6(*a*), practically ceases to exist at $\phi = 0.33$ near rotating stall; see Figs. 3(*b*) and 6(*b*). A reverse flow arises in the tip region; see the diagram for the relative velocity vectors at tip clearance ($r/r_t = 1.0058$), Fig. 6(*b*).

2 On the verge of rotating stall ($\phi = 0.33$) in Fig. 3(*b*), the region of low-energy fluid becomes thicker at the casing and thinner at the hub.

3 The higher the solidity of the cascade, the heavier the rotating stall in the form of a very steep pressure drop (Figs. 2(*a*) and 2(*b*)).

4 The narrower the tip clearance, the more severe the rotating stall (also see Figs. 2(*a*) and 2(*b*)).

5 A front can be detected between the forward and the reverse flow in the diagram of the relative velocity vectors in the tip clearance ($r/r_t = 1.0058$) near stall ($\theta = 0.33$) in Fig. 6(*b*).

These experimental results can be explained by means of the theory established by the discussers (1987, 1989), according to which rotating stall is introduced by secondary recirculations *r–f* and *m* in the meridional plane and around each of the blades (i.e., from the corner "pressure-side/hub" to the corner "suction-side/casing" of the neighboring blade channel); see Fig. 14. The reverse flow component *r* and the forward flow component *f* of the secondary recirculation in the meridional plane make the boundary layer on the casing thick due to deceleration, and the one on the hub thin due to acceleration. This explains the phenomenon in point 2 given above.

The reverse flow *r* then blocks the blade tip clearance and prevents generation of the leakage jet, as given in point 1. The narrower the tip clearance, the more severe the blocking. Therefore, a stronger rotating stall arises in the case of a narrow tip clearance, as shown in point 4.

In the diagram for the relative velocity vectors in the annular space of the tip clearance ($r/r_t = 1.0058$) in Fig. 6, the velocity vectors clearly show the leakage jet directed from the pressure side to the suction side of the blade at the normal operating point $\phi = 0.5$ in Fig. 6(*a*). Its strength increases from the inlet to the outlet because of the increasing pressure gradient across the blade tip. A strong forward flow prevails in the whole annular space from the inlet to the outlet region.

At the operating point of $\phi = 0.33$ near rotating stall in Fig. 6(*b*), however, the weak forward flow is still maintained at the inlet edge. But a little downstream at 1/5 of the blade chord, the flow becomes reverse on the suction side and is stagnated to practically zero on the pressure side of the blade. Farther downstream beyond 2/5 of the blade chord, the flow streams completely in the reverse direction. A front *p* between the forward and reverse flows, similar to the polar front at the midlatitude on the earth, can be drawn in the annular space between the inlet and 1/5 of the blade chord as given in Fig. 15(*b*). This front corresponds to the finding of the discussers (1987) by means of injecting colored dye through the casing into the flow. It is this front between two flows with different entropy (high entropy in the reverse flow and low entropy in the forward flow) that develops into a wavy motion because of the baroclinic instability.

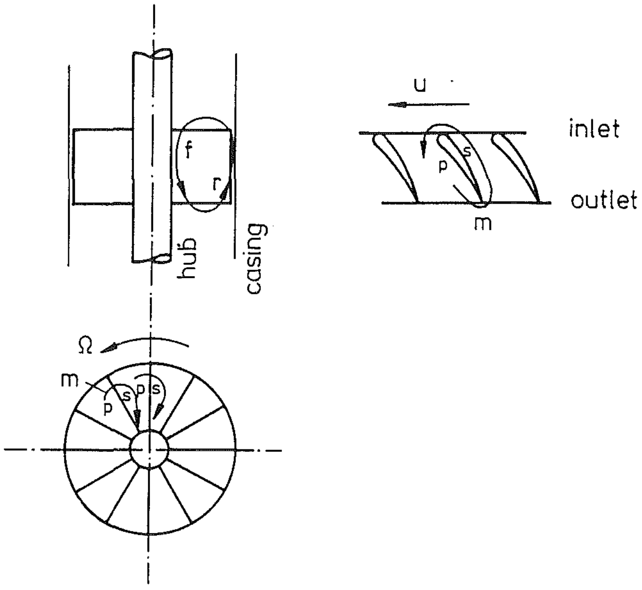

**Fig. 14 Secondary recirculations in the meridional plane (*f–r*) and around each of the blades (*m*) on the verge of rotating stall**

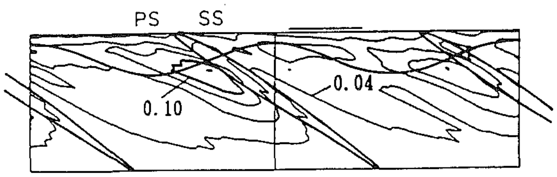

Pressure fluctuation

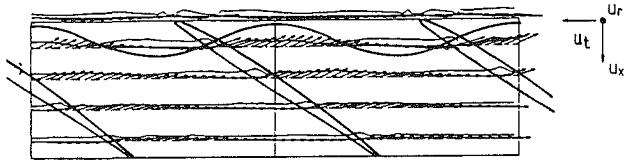

Relative velocity vectors ($r/r_t = 1.0058$)

**Fig. 15 Front between the forward and reverse flows in the annular space of the tip clearance (*b*) and in relationship with the pressure fluctuations (*a*), at the operating point of $\theta = 0.33$ near rotating stall**

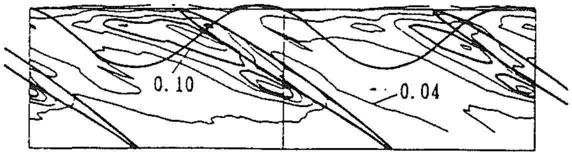

Pressure fluctuation

**Fig. 16 Front between the forward and reverse flows in the annular space of the tip clearance in relationship with the pressure fluctuations on the verge of rotating stall ($\theta = 0.324$)**

The field of the maximum pressure fluctuation given in Fig. 6(*b*) is shown in Fig. 15(*a*) in addition to this wavy front. We can detect that its main region coincides with the reverse flow zone onto the front. The strong fluctuation appears to be caused by the activity of the baroclinic instability in combination with the separation of the reverse flow into vortex filaments (see the 1989 paper of the discussers). These two effects are thus especially strong on the pressure side of the blade. This special fact can therefore be evaluated from the experiment of the present paper. The low-pressure trough on the suction surface of the blade in the leading edge region (see Fig. 6(*b*)) is the nose bubble of the incoming flow. This nose bubble deflects the flow toward the tangential direction, inducing the secondary recirculations given in Fig. 14, according to the discussers (1989).

---

[1] Sulzer Brothers Ltd., Winterthur, Switzerland.

[2] Institute for Turbomachinery, University of Hannover, Hannover, Federal Republic of Germany.

When the flow rate is further decreased to the verge of rotating stall, the field of the maximum pressure fluctuation extends farther downstream; see Fig. 7(*b*). This indicates that the wavy front has grown to a larger amplitude to accommodate this field; see Fig. 16. This wavy front is finally developed into a very low-frequency wave (see Chen, 1990) guiding the rotating stall as shown in Fig. 10 for rotor A at $\phi = 0.324$. This low-frequency wave is the Rossby wave, as described in the papers of the discussers (1987, 1990a).

The secondary flow behind the rotor near rotating stall ($\phi = 0.33$) in Fig. 6(*b*) exhibits a vortex, which coincides with the main path of the reverse flow shown in the diagram of the relative velocity vectors in the tip clearance region ($r/r_t = 1.0058$), as referred to previously. Then, *this vortex is a vortex* sink as determined by the discussers in a recent paper (1990b). Therefore, the main reverse flow is guided by a longitudinal vortex, because of the vortex-filament nature of the reverse flow, according to the discussers (1989).

According to the investigation of the discussers (1990a), the rotating stall is associated with a circular von Karman vortex street rotating with the stall cell. The higher the solidity of the cascade, the stronger the von Karman vortex can be generated according to the experiment of Kriebel et al. (1960). Therefore, we have a very deep rotating stall in the case of a large solidity, which is manifested in point 3 given previously.

## References

Chen, Y. N., Haupt, U., and Rautenberg, M., 1987, "On the Nature of Rotating Stall in Centrifugal Compressors With Vaned Diffusers, Part II: Karman Vortices as the Controlling Mechanism," *Proceedings of the 1987 Tokyo International Gas Turbine Congress*, pp. II 169-182.

Chen, Y. N., Haupt, U., and Rautenberg, M., 1989, "The Vortex-Filament Nature of Reverse Flow on the Verge of Rotating Stall," ASME JOURNAL OF TURBOMACHINERY, Vol. 111, pp. 450-461.

Chen, Y. N., 1990, "Rotating Stall in Radial Compressors and Pumps as Rossby Waves Associated With Transient Vortices," *Sulzer Technical Review*, No. 1, pp. 51-56.

Chen, Y. N., Haupt, U., and Rautenberg, M., 1990a, "Rossby Waves and Associated Transient Rotating Stall Vortices in Radial and Axial Turbo-compressors," *Zeitschrift für Flugwissenschaften und Weltraumforschung*, Vol. 14, No. 4, Aug.

Chen, Y. N., Haupt, U., and Rautenberg, M., 1990b, "Reverse Flow, Tip Leakage and Secondary Recirculations of Rotating Stall in Rotors/Impellers," *Proceedings of the 3rd International Congress of Fluid Mechanics*, Cairo, pp. 1549-1563.

Kriebel, A. R., Seidel, B. S., and Schwind, R. C., 1960, "Stall Propagation in a Cascade of Airfoils," NASA Report R-61.

## Authors' Closure

The authors acknowledge Drs. Chen, Haupt, Seidel, and Rautenberg for giving a unique interpretation upon the present experimental results.

In the authors' opinion, the secondary recirculations in Fig. 14 do not bring about the flow phenomena in Figs. 3(*b*) and 6(*b*), but are produced as a result of the flow phenomena whose mechanism can be more physically explained by Inoue et al. (1990). However, this may be a which-came-first-the-chicken-or-the-egg question.

The authors also cannot make a hasty conclusion for the existence of wavy patterns in Figs. 15 and 16. If they exist, it will be necessary to find another mechanism to change from a short wave mode to a longer one. The rotating stall should be a long wave mode that covers several blade passages.

In any case, investigation to elucidate more clearly the mechanism of rotating stall inception should be continued by many researchers.